

Biosorption of Methylene Blue and Orange II on deactivated *lichen Parmotrema dilatatum* : Modeling and kinetic studies

¹Kouassi Kouadio Dobi-Brice, ¹Ekou Lynda, ¹Ekou Tchirioua, ¹Yacouba Zoungran

¹Department of Chemistry, University of Nangui Abrogoua(LTPCM), 02 Bp 801 Abidjan 02, Ivory Cost

¹Department of Chemistry, University of Nangui Abrogoua(LTPCM), 02 Bp 801 Abidjan 02, Ivory Cost

¹Department of Chemistry, University of Nangui Abrogoua(LTPCM), 02 Bp 801 Abidjan 02, Ivory Cost

¹Department of Chemistry, University of Nangui Abrogoua(LTPCM), 02 Bp 801 Abidjan 02, Ivory Cost

Correspondence Author: Lynda Ekou, Department of Chemistry, University of Nangui Abrogoua (LTPCM), 02 Bp 801 Abidjan 02, Ivory Cost
E-mail: ekou_lynda@yahoo.fr

Received date: 15 November 2018, **Accepted date:** 20 December 2018, **Online date:** 31 December 2018

Copyright: © 2018 Kouassi Kouadio Dobi-Brice *et al*, This is an open-access article distributed under the terms of the Creative Commons Attribution License, which permits unrestricted use, distribution, and reproduction in any medium, provided the original author and source are credited.

Abstract

The flowering of industrial activities is generally accompanied by a phenomenon of effluent discharges containing many dangerous chemical substances. These water pollutants include Methylene Blue (BM) and Orange II (OII), which can cause human health problems and disrupt the balance of the aquatic system. Several effluent treatment methods exist but remain expensive and therefore inaccessible for developing countries such as Côte d'Ivoire.

The present work aims at the adsorption removal of these two toxic dyes on inexpensive plant biomass in this case deactivated lichens.

The various parameters influencing the adsorption such as the contact time, the initial concentration of the solution and the temperature, were studied. The kinetic study has shown that the biosorption process of BM and OII suitably follows pseudo-order two kinetics. The adsorption isotherms have shown that biosorption of BM is best described by the Freundlich model and that of OII by the Langmuir model. The thermodynamic study of the lichen-dye system showed that the adsorption process of the two dyes is spontaneous, endothermic for BM and exothermic for OII. The results obtained suggested a process of chemisorption and physisorption.

These results show the possibility of treatment of colored effluents by lichens.

Key words: lichens, biosorption, Methylene Blue, Orange II.

INTRODUCTION

In most developing countries, particularly in Côte d'Ivoire, aquatic environment contamination by pollutants from the textile, agrochemical and pharmaceutical industries is widespread. Methylene Blue and Orange II are among these harmful substances that are used in textile (cotton, wood, silk and paper) (Bhuiyan *et al.*, 2017), pharmaceutical industry (Pérez-Ibarbia *et al.*, 2016). Their release in aquatic system is undesirable, not only because of their color, but products resulting from degradation are toxic, carcinogenic or mutagenic (Croce *et al.*, 2017). Indeed, these pollutants can cause gastrointestinal irritation in humans with nausea, vomiting and diarrhea (Dulce *et al.*, 2017; Jabs and Drutz, 2001). In plants, they affect negatively the process of photosynthesis (Tahir *et al.*, 2016). Various methods such as electrochemical oxidation (Nidheesh *et al.*, 2018), ozonation (Wijannarong *et al.*, 2013), electrocoagulation (Pirkarami and Olya, 2017), photo process Fenton (Sohrabi *et al.*, 2017), nanofiltration, reverse osmosis (Nataraj *et al.*, 2009), etc. are used in order to remove these substances from wastewater. These methods are expensive and have revealed limitations in their use due to the production of toxic products.

Biosorption is an alternative technology for the removal of a wide range of pollutants from aquatic areas. This technology involves the use of natural or artificial adsorbents such as sawdust (Dulman and Cucu-Man, 2009), activated carbon (Baysal *et al.*, 2018), clay (Kausar *et al.*, 2018), peanut shell (Liu *et al.*, 2018), nanofiber membranes (Mousavi *et al.*, 2018) alumina, silica (Kannan *et al.*, 2008), banana peel (Munagapati *et al.*, 2018) and orange peel (Arami *et al.*, 2005) all derived from biomass. This approach has several advantages including a low cost due to the abundance of biomass, high selectivity efficiency regeneration with high yields. Lichens are plants resulting from the symbiotic association between an algae and a mushroom. Because of their high capacity of accumulation and retention of a wide variety of pollutants, they are widely used as indicators both of air quality and the environment health (Chatenet and Botineau, 2001).

In the present study, it is a question of carrying out the adsorption of Methylene Blue and Orange II on deactivated lichen biomass. The influence of contact time, initial dye concentration and temperature on lichens adsorption capacity of was studied.

1 MATERIALS AND METHODS

1.1. Sampling

The thalli of the lichen *Parmotrema dilatatum* were collected in the forest reserve of the LAMTO ecological station (5.02 ° C West and 6.13 ° C North). This reserve is 174 km far from the city of Abidjan (Ivory Coast) and located on the Abidjan-Yamoussoukro axis, between Singrobo and Taabo, and stretches along the Bandama River. This space is a natural Park of 2500 ha, with a tropical climate. The average temperature per year is about 28.28 ° C. The annual precipitation is around 1194 mm and the rate of humidity is higher than 58%. Once the lichens were harvested, they were immediately placed in envelopes made with paper in order to avoid transpiration of the vegetal matter and then sent to the laboratory.

In laboratory, lichens are removed from their substrates and then cleaned manually to remove rubbish such as soil, leaves, dust or insects. Thalli were then softly well washed with distilled water. An appropriate quantity of lichens was placed in an oven at 80 ° C during 48 hours in order to deactivate them. The deactivated lichens were completely ground and sieved and the diameters of the particles those size belonging to the interval 125-250 µm is used in all experiments.

1.2. Dyes preparation

0.1g of Methylene Blue (C₁₆H₁₈ClN₃S, Cl 52015, molecular weight = 319.85g / mol, λ_{max} = 664nm), and Orange II (C₁₆H₁₁N₂O₃Na, Cl 15510, molecular weight = 350.32 g / mol, λ_{max} = 582 nm) are dissolved in a 2000 ml flask and then completed with distilled water in order to have an initial concentration of 50 mg/L for each colored solution. Dilution of the initial solutions permit to obtain the different desired concentrations.

The chemical structures of dyes are given in Figure 1.

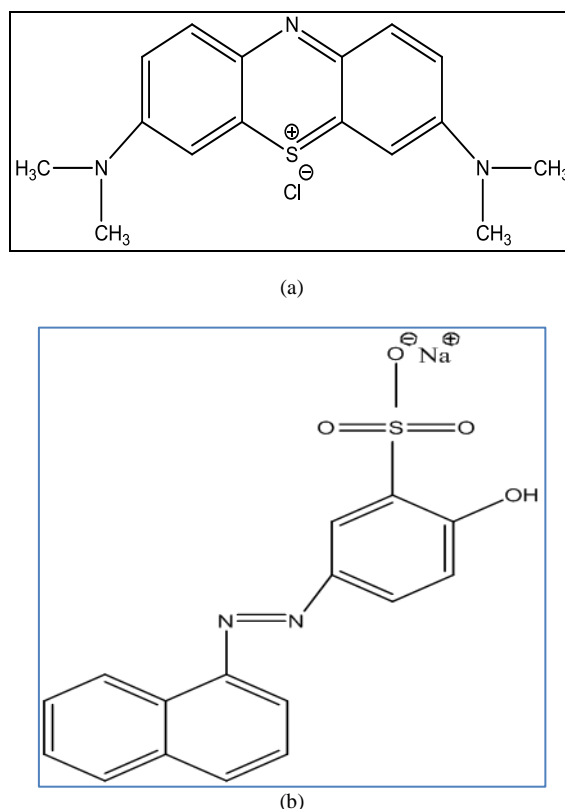


Figure 1 : Chemical structures of BM (a) and OII (b)

1.3. Biosorption studies

The contact time study was carried out by stirring the mixture 5 to 200 min. The initial dye concentration (10 - 500 mg/L) effect for BM and (5 - 50 mg / L) for OII was also studied. The effect of temperature has been studied by varying temperature (20 - 60°C) to determine the thermodynamic parameters. The optical densities were read using a UV / visible spectrophotometer (WFJ-752).

The amount biosorbed dye per gram of biomass at equilibrium (mg.g⁻¹) was calculated by using the following relationship (Jin et al., 2008) :

$$q_e = \frac{C_0 V_0 - C_e V}{m}$$

Where C₀ (mg/L) is the initial dye concentration, C_e (mg/L) the equilibrium dye concentration, V₀ and V are respectively the initial and final volume (L) of the solution and m the quantity (mg) of used lichens.

1.4 Statistical analysis

All calculation was performed with Microsoft office Excel 2013 Professional (Microsoft Corporation, WA, and USA). Mean values and standard errors were determined from three individual measurements.

2. RESULTS AND DISCUSSION

2.1. Kinetic models of biosorption

In order to characterize adsorption kinetics of BM and OII on deactivated lichens, experimental kinetic data were applied to the kinetic model of pseudo-first order of Lagergren model (Lagergren, 1898) and pseudo-second order kinetics proposed by Ho and McKay (Ho and McKay, 1999). These models are respectively described by the following relations (1) and (2) :

$$\frac{dq}{dt} = k_1 (q_e - q_t) \quad (1)$$

$$\frac{dq}{dt} = k_2 (q_e - q_t)^2 \quad (2)$$

The Integration of equations (1) and (2) by respecting the boundary conditions which are : $q_t=0$ at $t = 0$ and $q_t=q_t$ at $t=t$, leads to relations (3) and (4):

$$\ln(q_e - q_t) = \ln(q_e) - k_1 t \quad (3)$$

$$\frac{t}{q_t} = \frac{1}{k_2 q_e^2} + \frac{1}{q_e} t \quad (4)$$

Where k_1 (min⁻¹) and k_2 (g.mg⁻¹min⁻¹) are respectively the pseudo-first and pseudo-second order constants and q_t the quantity of biosorbed dye at a given time t .

The kinetic parameters of pseudo-first order and pseudo-second order were calculated from the respective graph plots $\ln[(q_e - q_t) = f(t)]$ and $t/q_t = f(t)$ (Fig. 2).

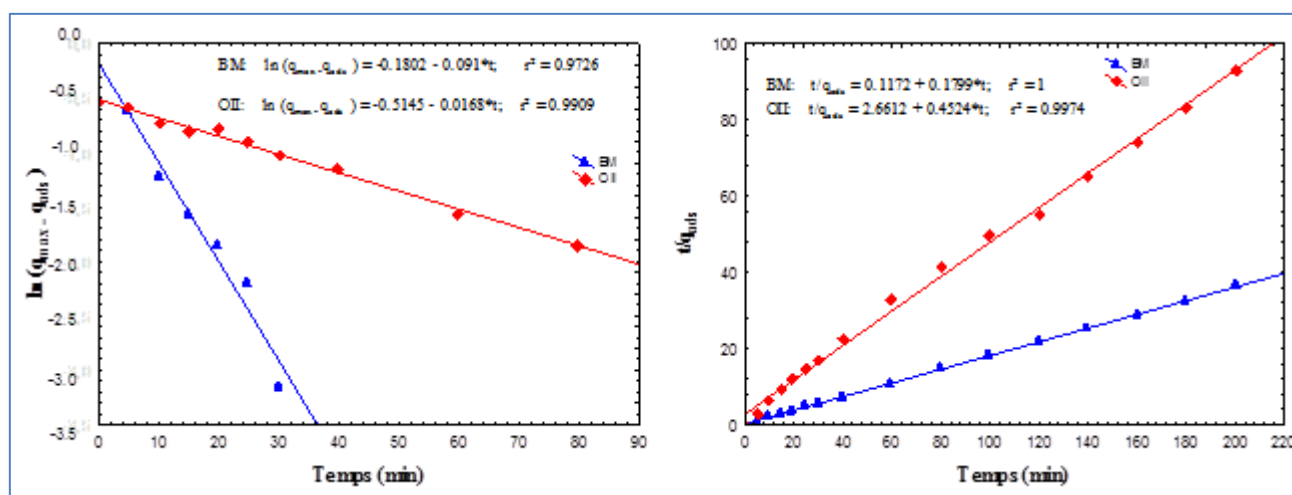


Figure 2 : Pseudo-first order (a) and pseudo-second order (b) models of BM and OII biosorption.

The results of the parameters calculation (k , q_e , r^2) are presented in Table 1. The analysis of this table shows that the correlation coefficients r^2 (0.9726, 0.9909) for the kinetic model of the pseudo-first order respectively for the BM and the OII, are relatively weaker than those of the pseudo-second order (1 ; 0.9974).

Table 1: Kinetic parameters ($q_{e,exp}$ (mg/g), $q_{e,theo}$ (mg/g), k_1 (min⁻¹) and k_2 (g/mg.min) of pseudo-first order and pseudo-second order models (mean± standard deviation)

	Pseudo-first order				Pseudo- second order			
	$q_{e,theo}$	$q_{e,exp}$	k_1	r^2	$q_{e,theo}$	$q_{e,exp}$	k_2	r^2
BM	0.185 ± 0.003	5.533 ± 0.002	0.067 ± 0.003	0.887 ± 0.001	5.556 ± 0.003	5.533 ± 0.002	0.844 ± 0.001	1 ± 0.000
OII	0.649 ± 0.005	2.159 ± 0.003	0.014 ± 0.003	0.983 ± 0.002	2.244 ± 0.003	2.159 ± 0.003	0.053 ± 0.001	0.998 ± 0.001

In addition, the theoretical values ($q_{e,theo}$) computed from the pseudo-second-order model showed good agreement with the experimental values ($q_{e,exp}$) compared to those of the pseudo-first order. Although the condition $r^2 \geq 0.9$ is satisfied for both models, the difference between the values ($q_{e,theo}$) and ($q_{e,exp}$) allows to conclude that the biosorption of the BM and OII dyes on the deactivated lichen *Parmotrema dilatatum* is the kinetic of the pseudo -second order. These results are in agreement with those of Bentahar *et al.* (2017), and Jin *et al.* (2014) respectively in the adsorption of BM on powdered nut shells and OII on a zeolite coated with surfactant.

2.2. Adsorptions isotherms

Several adsorption isotherm models have been developed to describe these different interactions. In this study, Freundlich, Langmuir and Dubinin-Radushkevich (D-R) models were applied to the experimental data.

Langmuir isotherm involves monolayer adsorption on a surface containing homogeneous adsorption sites, without transmigration of adsorbates and without any interaction between the adsorbed molecules (Demirkiran, 2015). Once a site is occupied, no additional adsorption can take place, resulting in saturation of the surface (Kono and Kusumoto, 2015).

The Langmuir isotherm is translated by the following relation (Langmuir, 1918) :

$$\frac{C_e}{q_e} = \frac{1}{q_{max} K_L} + \frac{C_e}{q_{max}} \tag{5}$$

Where q_{max} (mg/g) is the maximum dye biosorption corresponding to the saturation capacity and K_L is the Langmuir constant. In this work the application of experimental data to the Langmuir model is given in Figure 3.

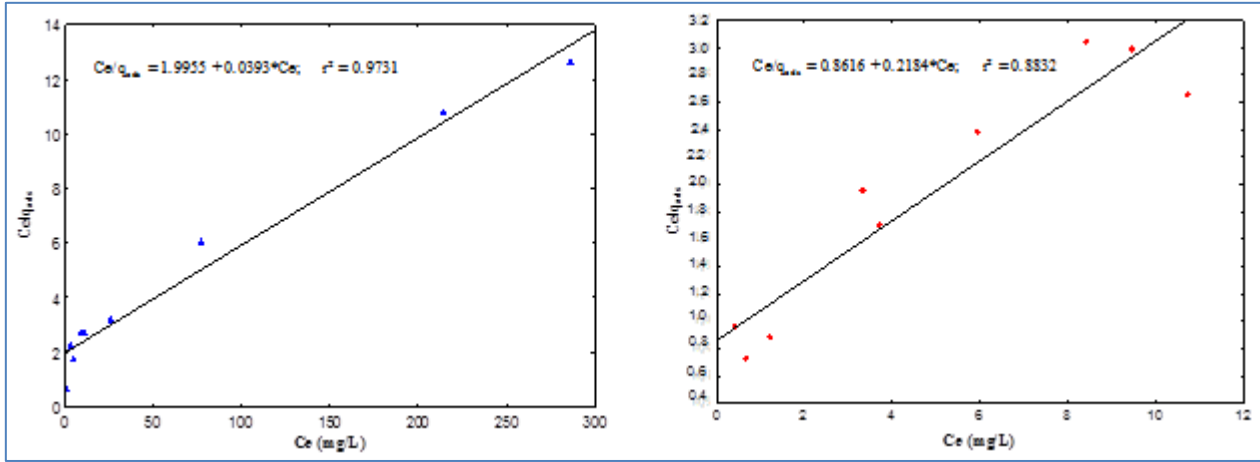


Figure 3 : Langmuir isotherm of adsorption of BM (a) and OII (b)

Freundlich model is based on the assumptions that adsorption is not limited to monolayer formation, hence a multilayer adsorption with active sites are not evenly distributed on the surface of the adsorbent (Mohamed et al., 2018). The Freundlich adsorption isotherm can be expressed by the following relation (Freundlich, 1906):

$$\ln(q_e) = \ln(K_F) + \frac{1}{n} \ln(C_e) \tag{6}$$

Where K_F (L/g) is the Freundlich constant linked to biosorption capacity and n is an empirical parameter that reports the intensity of biosorption and varies with the heterogeneity of the vegetal matter (Gorgulu Ari and Celik, 2013). The application of experimental data to the Freundlich model is given in Figure 4.

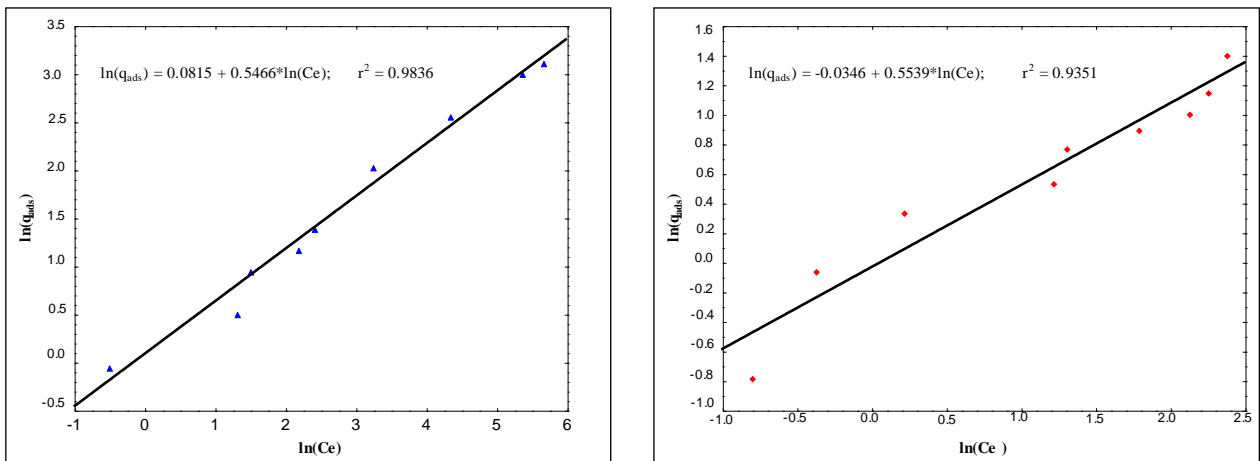


Figure 4 : Freundlich isotherm of adsorption of BM (a) and OII (b)

The Dubinin-Radushkevich isotherm is used to determine the physical or chemical nature of the biosorption processes of the dyes on the lichen *Parmotrema dilatatum*. The linear form of the D-R isotherm equation (Dubinin et al., 1947) is given by the following equation (7) :

$$\ln(q_e) = \ln(q_{max}) - \beta E^2 \tag{7}$$

Where q_e is the quantity of adsorbed dyes per gram of biomass at equilibrium (mol/L), q_{max} is the maximum biosorption capacity (mol/g), β is the activity coefficient related to the average energy of biosorption (mol² / J²) and E is the potential of Polanyi defined by the following relation: The average biosorption energy provides information about the biosorption mechanism. It is obtained by the relation given below :

$$\varepsilon \text{ (kJ/mol)} = \frac{1}{\sqrt{(-2\beta)}} \tag{8}$$

The application of the experimental data to the Freundlich model is given in Figure 5.

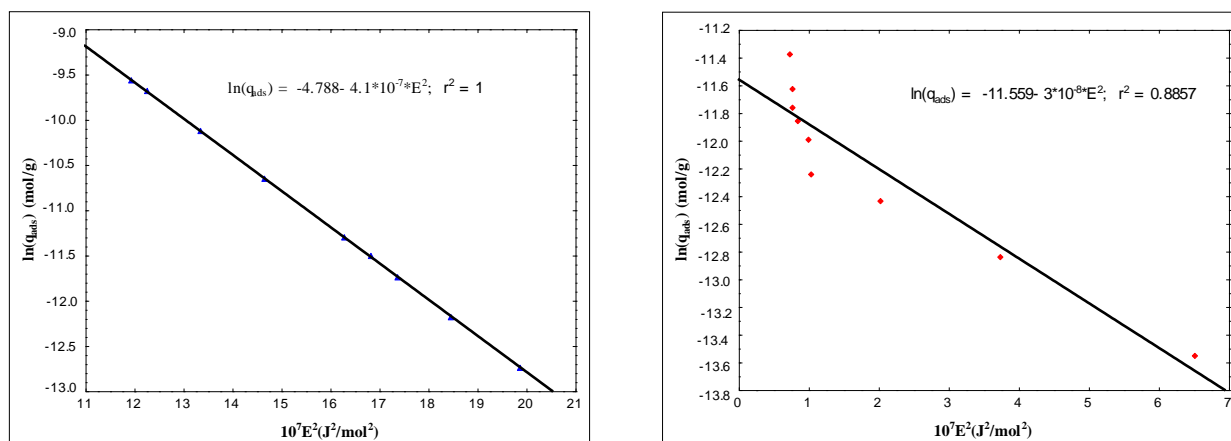


Figure 5 : Dubinin-Radushkevich adsorption isotherm of BM (a) and OII (b).

Constants derived from the model Langmuir, Freundlich and Dubinin-Radushkevich equations are gathered in Table 2.

Table 2 : BM and OII adsorption parameters (mean \pm standard deviation) on deactivated lichen according to Langmuir, Freundlich and Dubinin-Radushkevich (D-R) models.

	Langmuir			Freundlich			Dubinin-Radushkevich		
	Qmax(mg/g)	KL(L/mg)	r ²	1/n	KF(L/g)	r ²	Qmax(mol/g)	E(kJ/mol)	r ²
B	25.445 \pm 0.003	0.020 \pm 0.003	0.999 \pm 0.00	0.547 \pm 0.005	1.085 \pm 0.003	0.984 \pm 0.003	(8.329 \pm 0.009)*10-3	1.118 \pm 0.008	0.999 \pm 0.001
OII	4.579 \pm 0.002	0.254 \pm 0.004	0.886 \pm 0.004	0.554 \pm 0.003	0.966 \pm 0.005	0.935 \pm 0.007	(9.549 \pm 0.003)*10-6	4.082 \pm 0.003	0.886 \pm 0.002

The values of the constant $1/n$ of Freundlich isotherm are 0.5466 and 0.5539 respectively for BM and OII. This result means that the adsorption of BM and OII on the deactivated lichen is favorable.

The correlation coefficients of Langmuir isotherm of Methylene Blue and Orange II are 0.9989 and 0.8857 respectively. For Freundlich isotherm, the coefficients are 0.9836 and 0.9351 respectively for BM and OII (Table 2). A comparison of these coefficients shows that biosorption of BM is well described by Langmuir model and that of OII by Freundlich model.

The calculated values of the mean energy of biosorption (E) are 1.118 and 4.082 kJ / mol respectively for BM and OII. These values are all less than 8 kJ / mol with high correlations. This result suggests that the adsorption of BM and OII dyes are all physisorption processes (Gorgulu Ari and Celik, 2013; Mohamed et al., 2018).

2. 3. Thermodynamic study

Thermodynamic parameters : Enthalpy ΔH° , Entropy ΔS° and Free Energy ΔG° were determined experimentally. The experimental results were applied to the following equations (9) and (10) (Elmoubarki et al., 2015):

$$\Delta G_0 = -RT \ln KD \quad (9)$$

$$\ln(KD) = \frac{[\Delta S]^\circ}{R} - \frac{[\Delta H]^\circ}{RT} \quad (10)$$

Where $KD = q_e/C_e$ is the distribution coefficient, R (8.314 J. mol⁻¹.K⁻¹) is the perfect gas constant, T (K) is the temperature of the solution.

The plot of the graph $\ln(KD) = f(1/T)$ (Fig. 8) allowed to determine ΔH° , ΔS° and ΔG° . The results are summarized in Table 3 below.

Table 3: Thermodynamic parameters (mean \pm standard deviation), for BM and OII adsorption.

T(K)	ΔG° (kJ/mol)		ΔH° (kJ/mol)		ΔS° (J/mol)	
	BM	OII	BM	OII	BM	OII
293	-70.439 \pm 0.006	-3.021 \pm 0.003	8.752 \pm 0.012	-24.299 \pm 0.007	30.213 \pm 0.006	-72.180 \pm 0.04
303	-539.143 \pm 0.005	-2.564 \pm 0.004				
313	-602.858 \pm 0.008	-1.858 \pm 0.008				
323	-904.731 \pm 0.007	-0.828 \pm 0.004				
333	-1406.905 \pm 0.022	-0.261 \pm 0.006				

The values of Gibbs free energy variation (ΔG°) are all negative which means that the adsorption processes of BM and OII are spontaneous and therefore favorable, thus reflecting the affinity of the deactivated lichens for the cations and anions of dye (Vimonses et al., 2009; Pal et al., 2015).

The enthalpy of biosorption is -24.3 for OII. This negative value indicates the exothermic nature of the adsorption process which means that the adsorption of OII is favored by a decrease of the temperature (Toor and Jin, 2012).

The enthalpy of biosorption of BM is 2.57. The adsorption is endothermic and favorable by rising of temperature (Guyo et al., 2017; Güzel et al., 2015). Zhang et al have found the similar result (Zhang et al., 2013) which the positive value of $[\Delta H]^\circ$ indicating the endothermic nature of adsorption of Methylene Blue on diatomite at different temperatures.

The value of ΔS° is 9.5 kJ / mol for the BM, this positive value suggests an increase in the disorder at the lichen/solution interface during adsorption (Ngulube *et al.*, 2017). The negative value of OII indicates a decrease of disorder at the adsorbent / solution interface. This adsorption does not bring any change to the structure of the lichen *Parmotrema dilatatum* (Kalev and Toor, 2018; Li *et al.*, 2017).

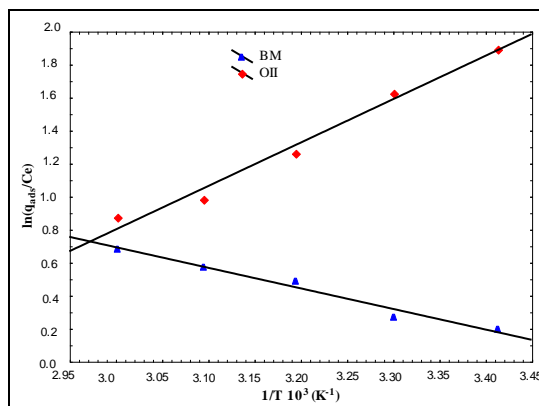


Figure 6 : Effect of temperature on sorption of BM and OII.

CONCLUSION

This study showed that lichen *Parmotrema dilatatum* deactivated can be used successfully as an effective adsorbent for the removal of Methylene Blue and Orange II. The kinetics of biosorption of the two dyes is perfectly described by kinetics of pseudo-second order. The biosorption isotherm is well adjusted by Langmuir equation in the case of BM and Freundlich equation in the case of the OII. Thermodynamic studies have shown that adsorption is spontaneous for the two kinds of dyes, endothermic for BM and exothermic for OII and it leads to greater entropy in the case of BM and lower entropy in the case of OII.

REFERENCES

- Arami, M., N. Y. Limae, N. M. Mahmoodi, and N. S. Tabrizi, 2005. Removal of dyes from colored textile wastewater by orange peel adsorbent: Equilibrium and kinetic studies. *J. Colloid Interface Sci.*, 288: 371–376. doi:10.1016/J.JCIS.2005.03.020.
- Baysal, M., K. Bilge, B. Yılmaz, M. Papila, and Y. Yürüm, 2018. Preparation of high surface area activated carbon from waste-biomass of sunflower piths: Kinetics and equilibrium studies on the dye removal. *J. Environ. Chem. Eng.*, 6: 1702–1713. doi:10.1016/J.JECE.2018.02.020.
- Bentahar, S., A. Dbik, M. El Khomri, N. El Messaoudi, and A. Lacherai, 2017. Adsorption of methylene blue, crystal violet and congo red from binary and ternary systems with natural clay: Kinetic, isotherm, and thermodynamic. *J. Environ. Chem. Eng.*, 5: 5921–5932. doi:10.1016/J.JECE.2017.11.003.
- Bhuiyan, M.A.R., A. Islam, A. Ali, and M. N. Islam, 2017. Color and chemical constitution of natural dye henna (*Lawsonia inermis* L) and its application in the coloration of textiles. *J. Clean. Prod.*, 167: 14–22. doi:10.1016/J.JCLEPRO.2017.08.142.
- Chatenet, P., and M. Botineau, 2001. Utilisation des lichens dans la mise en évidence des éléments traces présents dans les cours d'eau. *Cryptogam. Mycol.*, 22: 225–237. doi:10.1016/S0181-1584(01)01063-6.
- Croce, R., F. Cinà, A. Lombardo, G. Crispeyn, C.I. Cappelli, M. Vian, S. Maiorana, E. Benfenati, D. Baderna, 2017. Aquatic toxicity of several textile dye formulations: Acute and chronic assays with *Daphnia magna* and *Raphidocelis subcapitata*. *Ecotoxicol. Environ. Saf.*, 144: 79–87. doi:10.1016/j.ecoenv.2017.05.046.
- Demirkiran, N., 2015. Copper adsorption by natural manganese dioxide. *Trans. Nonferrous Met. Soc. China*, 25: 647–653. doi:10.1016/S1003-6326(15)63648-2.
- Dubinin, M.M., E. D. Zaverina, and L. V. Radushkevich, 1947. Sorption et structure des charbons actifs. *Adsorption des vapeurs organiques. Zhurnal Fiz. Khimii*, 21: 1351–1362.
- Dulce, R.A., S. Kulandavelu, I. H. Schulman, J. Fritsch, and J. M. Hare, 2017. Nitric Oxide Regulation of Cardiovascular Physiology and Pathophysiology, in: *Nitric Oxide*. Elsevier, pp: 313–338. doi:10.1016/B978-0-12-804273-1.00024-7.
- Dulman, V. and S. M. Cucu-Man, 2009. Sorption of some textile dyes by beech wood sawdust. *J. Hazard. Mater.*, 162: 1457–1464. doi:10.1016/J.JHAZMAT.2008.06.046.
- Elmoubarki, R., F.Z. Mahjoubi, H. Tounsadi, J. Moustadraf, M. Abdennouri, A. Zouhri, A. El Albani, N. Barka, 2015. Adsorption of textile dyes on raw and decanted Moroccan clays: Kinetics, equilibrium and thermodynamics. *Water Resour. Ind.*, 9: 16–29. doi:10.1016/j.wri.2014.11.001.
- Freundlich, H.M.F., 1906. Über die adsorption in losungen. *Zeitschrift für Phys. Chemie-Leipzig*, 57: 385–470.
- Gorgulu Ari, A. and S. Celik, 2013. Biosorption potential of Orange G dye by modified *Pyraecanthia coccinea*: Batch and dynamic flow system applications. *Chem. Eng. J.*, 226: 263–270. doi: 10.1016/j.cej.2013.04.073.
- Guyo, U., N. Matewere, K. Matina, T. Nharingo, and M. Moyo, 2017. Fabrication of a sustainable maize stover-graft-methyl methacrylate biopolymer for remediation of methyl red contaminated waters. *Sustain. Mater. Technol.*, 13: 9–17. doi:10.1016/j.susmat.2017.05.001.
- Güzel, F., H. Saygılı, G. Akkaya Saygılı, and F. Koyuncu, 2015. New low-cost nanoporous carbonaceous adsorbent developed from carob (*Ceratonia siliqua*) processing industry waste for the adsorption of anionic textile dye: Characterization, equilibrium and kinetic modeling. *J. Mol. Liq.*, 206: 244–255. doi:10.1016/j.molliq.2015.02.037.
- Ho, Y.S. and G. McKay, 1999. Pseudo-second order model for sorption processes. *Process Biochem.* 34, 451–465.
- Jabs, C.F.I. and H.P. Drutz, 2001. The role of intraoperative cystoscopy in prolapse and incontinence surgery. *Am. J. Obstet. Gynecol.*, 185: 1368–1373. doi:10.1067/MOB.2001.119072.
- Jin, X., M. Jiang, X. Shan, Z. Pei, and Z. Chen, 2008. Adsorption of methylene blue and orange II onto unmodified and surfactant-modified zeolite. *J. Colloid Interface Sci.*, 328: 243–247. doi:10.1016/j.jcis.2008.08.066.
- Jin, X., B. Yu, Z. Chen, J.M. Arocena and R.W. Thring, 2014. Adsorption of Orange II dye in aqueous solution onto surfactant-coated zeolite: Characterization, kinetic and thermodynamic studies. *J. Colloid Interface Sci.*, 435: 15–20. doi:10.1016/j.jcis.2014.08.011.
- Kalev, S.D. and G.S. Toor, 2018. The Composition of Soils and Sediments, in: *Green Chemistry*. Elsevier, pp: 339–357. doi:10.1016/B978-0-12-809270-5.00014-5.
- Kannan, C., T. Sundaram and T. Palvannan, 2008. Environmentally stable adsorbent of tetrahedral silica and non-tetrahedral alumina for removal and recovery of malachite green dye from aqueous solution. *J. Hazard. Mater.*, 157: 137–145. doi:10.1016/J.JHAZMAT.2007.12.116.
- Kausar, A., M. Iqbal, A. Javed, K. Aftab, Z.-H. Nazli, H.N. Bhatti and S. Nouren, 2018. Dyes adsorption using clay and modified clay: A review. *J. Mol. Liq.*, 256: 395–407. doi:10.1016/J.MOLLIQ.2018.02.034.

- Kono, H. and R. Kusumoto, 2015. Removal of anionic dyes in aqueous solution by flocculation with cellulose ampholytes. *J. Water Process Eng.*, 7: 83–93. doi:10.1016/J.JWPE.2015.05.007.
- Lagergren, S., 1898. Zur Theorie der Sogenannten Adsorption Gelöster Stoffe, *Kungliga Svenska Vetenskapsakademiens. Handlingar* 24, 1–39.
- Langmuir, I., 1918. The adsorption of gases on plane surfaces of glass, mica and platinum. *J. Am. Chem. Soc.*, 40: 1361–1403. doi:10.1021/ja02242a004.
- Li, Z., Z. Jia, T. Ni and S. Li, 2017. Adsorption of methylene blue on natural cotton based flexible carbon fiber aerogels activated by novel air-limited carbonization method. *J. Mol. Liq.*, 242: 747–756. doi:10.1016/j.molliq.2017.07.062.
- Liu, J., Z. Wang, H. Li, C. Hu, P. Raymer, and Q. Huang, 2018. Effect of solid state fermentation of peanut shell on its dye adsorption performance. *Bioresour. Technol.*, 249: 307–314. doi:10.1016/J.BIORTECH.2017.10.010.
- Mohamed, S.K., S. H. Hegazy, N. A. Abdelwahab, and A. M. Ramadan, 2018. Coupled adsorption-photocatalytic degradation of crystal violet under sunlight using chemically synthesized grafted sodium alginate/ZnO/graphene oxide composite. *Int. J. Biol. Macromol.*, 108: 1185–1198. doi:10.1016/J.IJBIOMAC.2017.11.028.
- Mousavi, S., F. Deuber, S. Petrozzi, L. Federer, M. Aliabadi, F. Shahraki and C. Adlhart, 2018. Efficient dye adsorption by highly porous nanofiber aerogels. *Colloids Surfaces A Physicochem. Eng. Asp.*, 547: 117–125. doi:10.1016/J.COLSURFA.2018.03.052.
- Munagapati, V.S., V. Yarramuthi, Y. Kim, K. M. Lee, and D.-S. Kim, 2018. Removal of anionic dyes (Reactive Black 5 and Congo Red) from aqueous solutions using Banana Peel Powder as an adsorbent. *Ecotoxicol. Environ. Saf.*, 148: 601–607. doi:10.1016/J.ECOENV.2017.10.075.
- Nataraj, S.K., K. M. Hosamani, and T. M. Aminabhavi, 2009. Nanofiltration and reverse osmosis thin film composite membrane module for the removal of dye and salts from the simulated mixtures. *Desalination*, 249: 12–17. doi:10.1016/J.DESAL.2009.06.008.
- Ngulube, T., J. R. Gumbo, V. Masindi, and A. Maity, 2017. An update on synthetic dyes adsorption onto clay based minerals: A state-of-art review. *J. Environ. Manage.*, 191: 35–57. doi:10.1016/J.JENVMAN.2016.12.031.
- Nidheesh, P.V., M. Zhou, and M. A. Oturan, 2018. An overview on the removal of synthetic dyes from water by electrochemical advanced oxidation processes. *Chemosphere*, 197: 210–227. doi:10.1016/J.CHEMOSPHERE.2017.12.195.
- Pal, S., A.S. Patra, S. Ghorai, A.K. Sarkar, V. Mahato, S. Sarkar, R.P. Singh, 2015. Efficient and rapid adsorption characteristics of templating modified guar gum and silica nanocomposite toward removal of toxic reactive blue and Congo red dyes. *Bioresour. Technol.*, 191: 291–299. doi:10.1016/j.biortech.2015.04.099.
- Pérez-Ibarbia, L., T. Majdanski, S. Schubert, N. Windhab, and U. S. Schubert, 2016. Safety and regulatory review of dyes commonly used as excipients in pharmaceutical and nutraceutical applications. *Eur. J. Pharm. Sci.*, 93: 264–273. doi:10.1016/J.EJPS.2016.08.026.
- Pirkarami, A. and M.E. Olya, 2017. Removal of dye from industrial wastewater with an emphasis on improving economic efficiency and degradation mechanism. *J. Saudi Chem. Soc.*, 21: 179–186. doi:10.1016/J.JSCS.2013.12.008.
- Sohrabi, M.R., A. Khavaran, S. Shariati, and S. Shariati, 2017. Removal of Carmoisine edible dye by Fenton and photo Fenton processes using Taguchi orthogonal array design. *Arab. J. Chem.*, 10: 3523–3531. doi:10.1016/J.ARABJC.2014.02.019.
- Tahir, H., M. Sultan, N. Akhtar, U. Hameed, and T. Abid, 2016. Application of natural and modified sugar cane bagasse for the removal of dye from aqueous solution. *J. Saudi Chem. Soc.*, 20: 115–121. doi:10.1016/J.JSCS.2012.09.007.
- Toor, M., and B. Jin, 2012. Adsorption characteristics, isotherm, kinetics, and diffusion of modified natural bentonite for removing diazo dye. *Chem. Eng. J.*, 187: 79–88. doi:10.1016/j.cej.2012.01.089.
- Vimonses, V., S. Lei, B. Jin, C. W. K. Chow, and C. Saint, 2009. Kinetic study and equilibrium isotherm analysis of Congo Red adsorption by clay materials. *Chem. Eng. J.*, 148: 354–364. doi:10.1016/j.cej.2008.09.009.
- Wijannarong, S., S. Aroonsrimorakot, P. Thavipoke, charaporn Kumsopa, and S. Sangjan, 2013. Removal of Reactive Dyes from Textile Dyeing Industrial Effluent by Ozonation Process. *APCBEE Procedia*, 5: 279–282. doi:10.1016/J.APCBEE.2013.05.048.
- Zhang, J., Q. Ping, M. Niu, H. Shi, and N. Li, 2013. Kinetics and equilibrium studies from the methylene blue adsorption on diatomite treated with sodium hydroxide. *Appl. Clay Sci.*, 83 (84): 12–16. doi:10.1016/j.clay.2013.08.008.